Inorganic Chemistry

Communication

pubs.acs.org/IC

A Crown-Shaped 24-Molybdate Cluster Constructed by Organotriphosphonate Ligand

Lu Yang,[†] Pengtao Ma,[†] Zhen Zhou,[†] Jingping Wang,*[,†] and Jingyang Niu*[,†,‡]

[†]Henan Key Laboratory of Polyoxometalate Chemistry, Institute of Molecular and Crystal Engineering, College of Chemistry and Chemical Engineering, Henan University Kaifeng, Henan 475004, People's Republic of China

[‡]State Key Laboratory of Coordination Chemistry, Nanjing, Jiangsu, China

Supporting Information

ABSTRACT: A crown-shaped organic−inorganic hybrid polyoxomolybdate, $Na_5[H_7\{N(CH_2PO_3)_3\}Mo_6O_{16}(OH)(H_2O)_4]_4\cdot 18H_2O$ (**1**) has been presented and characterized. Such an intriguing structure consists of a 24-molybdenum-membered polyanion constructed by organotriphosphonate ligands, which represents the highest nuclearity of metal atoms in the area of organophosphonate-based polyoxometalates.

Polyoxometalates (POMs) are anionic polymetallic clusters of early transition metals (e.g., Mo, W, V, Nb, and Ta) usually in their highest oxidation state, incorporated with oxo ligands that exhibit versatile structures with different sizes and shapes.[1] These species are thus regarded as multifunctional materials for wide applications in medicine, electrochemistry, catalysis, and proton conductors.[2] Within this field, organophosphonates combined with POMs represent a large subclass and have received considerable attention, especially for diphosphonate-based POM derivatives, which have been fully explored on account of their potential properties.[3] The monophosphonate-functionalized polyoxomolybdates, generally, as a Strandberg type $[Mo_5O_{15}(O_3PR)_2]^{4-}$ (R = $CH_2C_6H_4NH_3$, $CH_2CH_2NH_3$, CH_3CH_2 etc.) polyanion, have also been explored for a long time.[4] In addition, there are plenty of examples based on both of these polyanions, which are further decorated by transition metals along with organic linkers to form high dimensional structures through hydrothermal syntheses.[5] However, reports on triphosphonato-POMs are really limited. The only example is based on vanadium oxides and 1,3,5-tris(phenyl)-4,4′-triphosphonic acid constructing a two-dimensional trinuclear $[V_3O_3(OH)\{C_6H_3(C_6H_4PO_3H)_3\}]$ cluster, which is linked through the triphosphonate ligand.[6] Thus, we decided to utilize amino trimethylene phosphonic acid (ATMP), as one of the representatives of organotrisphonates, to react with molybdenum. Unlike the aromatic triphosphonates that possess a rigid backbone, ATMP is more flexible in space morphology, which is a benefit for coordination. Compared with W and V, Mo atoms are easier to polymerize large POM compounds with high nuclearity.[7] To date, the highest nuclearity of metal atoms in organophosphonate-based POMs chemistry is 20-molybdophosphonate $[\{(Mo_2O_4)_{10}(O_3PCH_2PO_3)_{10}(HCOO)_{10}\}]^{30-}$, an ovoid cluster with two nonequivalent interconnected wheels, which contains six $\{Mo_2O_4(H_2O)_2\}$ dinuclear fragments forming the ring and another four groups in the wheels linked by formato ligands, while the carboxyl ligands are located inside of the cavity.[8]

Herein, we present the synthesis of an ATMP-based POMs derivative $Na_5[H_7\{N(CH_2PO_3)_3\}Mo_6O_{16}(OH)(H_2O)_4]_4\cdot 18H_2O$ (**1**) that exhibits a crown-shaped structure. To the best of our knowledge, compound **1**, as a 24-molybdenum-membered cluster, represents the highest nuclearity of metal atoms in organophosphonate-based POMs chemistry.

Compound **1** was isolated from aqueous solution as well-defined colorless stick crystals and prepared by mixing ATMP and $Na_2MoO_4\cdot 2H_2O$ in the presence of perchloric acid (pH value is around 0.7) and hydrogen peroxide, which plays a role in preventing the reduction of Mo(VI) ions in the reaction system. Single-crystal X-ray structural analysis shows that **1** crystallizes in the orthorhombic *Fddd* space group. Compund **1** is a macrocyclic triphosphonate-based polyoxomolybdate of large size and high symmetry by self-assembly. As shown in Figure 1, $[\{N(CH_2PO_3)_3\}Mo_6O_{16}(OH)(H_2O)_4]_4^{12-}$ (**1a**) can be described as a tetramer of four $[\{N(CH_2PO_3)_3\}Mo_6O_{17}(OH)(H_2O)_3]^{3-}$ units leading to an open cavity of about 6.0 Å × 6.7 Å in diameter, where we could not identify any guest ions or molecules, and an overall edge length of about

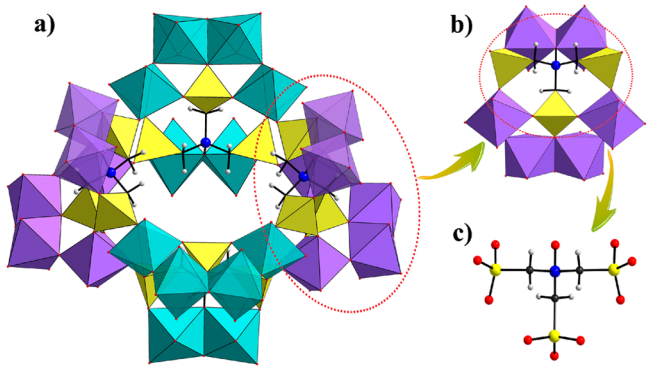

Figure 1. (a) Combined polyhedral/ball-and-stick representation of **1a**. (b) Combined polyhedral/ball-and-stick representation of the subunit. (c) Coordination mode of the ATMP ligand. Color code: N, blue; H, gray; MoO_6 octahedral, purple/aqua; and PO_3C tetrahedral, yellow.

Received: April 6, 2013
Published: July 17, 2013

   dx.doi.org/10.1021/ic400848r | *Inorg. Chem.* 2013, 52, 8285−8287

2 nm (Figure 2). As known, such a crown-shaped triphosphonate-incorporated POM has never been reported.

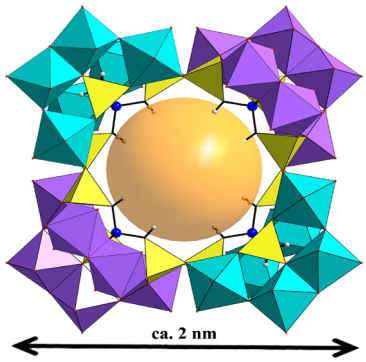

Figure 2. Structure of open cavity in **1a** along *a* axis.

The structure can be compared with the well-known polyoxoanion $[As_4W_{40}O_{140}]^{28-}$ that is assembled by four $[AsW_9O_{33}]^{3-}$ subunits connected by four other WO_6 bridging octahedra.[9] The ATMP is a multidentate ligand that shares all of the nine O atoms to coordinate in **1**. We observe that the N atom and two of the CH_2 groups from ATMP are exposed on the inside, while the other CH_2 group hides in the interlayer of the MoO_6 octahedra. In a unit, six Mo atoms are located in two layers: a dimer of MoO_6 octahedra on one side, while the four other Mo atoms are on in the other side, which present a saddle-shaped architecture. The Mo6 atom in each unit is disordered with 76%/24% site occupancy. Each PO_3 group of the ATMP ligand connects three MoO_6 octahedra, but one of the PO_3 has a μ_3−O bridging atom, which anchors to two Mo atoms, and the other two μ_2−O atoms bind to the Mo atoms on the same side. Thus, ATMP acts as a stanchion to support the combination of the tetrameric structure. In addition, the tetramers are connected by the alternate front−back type of fashion (represented by two colors), which is due to the steric hindrance effect. This type of connectivity mode is unusual in the family of organophosphonate-based POMs. The center N atom of each ATMP shows tetrahedron geometry defined by three C atoms in the ligand and a bridging O atom linking the two Mo atoms on the same side.

According to the bond valence sum (BVS) calculations, the oxidation of all P and Mo atoms are +3 and +6, respectively, and the results are further confirmed by XPS spectra (Supporting Information). The P−O bonds range between 1.500(6) and 1.546(5) Å in length, while the Mo−O bond lengths in the range of 1.682(7)−2.341(6) Å, with BVS calculations indicating two protons associated with the terminal oxygen atoms (O10, O16, O26, O29) and a singly protonated bridging oxo ligand (Mo−O27H). The O−Mo−O bond angles are between 70.5(2)°and 169.8(3)°. In **1a**, the P atoms are linking with Mo atoms via bridging μ_2− and μ_3−oxo ligands, thus the P−O−Mo bond angles, O−P−C angles, and O−P−O are in the range of 127.5(3)−137.6(3)°, 100.5(3)−111.1(3)°, and 108.5(3)−116.1(3)°, respectively. The structure of **1a** is extended to a two-dimensional layerwork by two Na^+ cations in each subunit. The packing arrangement results in another type void (B) with the cross-section sizes of 13.3 Å × 11.4 Å along the *a*-axis.

The behavior in solution of this cyclic compound has been investigated by ^{31}P NMR. The spectrum of **1** dissolved in D_2O at room temperature exhibits two resonances located at 3.49 and 6.28 ppm with relative intensity 2:1. The results are well consistent with the solid-state structure of the compound, which has two types of P atoms within a subunit. This spectrum can maintain about one day, and a resonance of unknown species at 4.66 ppm progressively increases, but the resonances attributed to **1** still exist (Figure S8, Supporting Information). In addition, the ^{31}P NMR spectra were performed at different pH values in the 0.6−4.2 range. With the changing of pH value from 2.2 to 0.6, the two resonances attributed to **1a** progressively decrease, while another resonance located at 4.62 ppm appears. When the pH increases, the intensity of resonance at 3.49 ppm gradually decreases. This trend continues until pH 4.2, and the resonance at 3.49 ppm totally disappears indicating the polyanion **1a** might be isolated. The ^{31}P NMR spectroscopic studies show that the skeleton of **1a** is stable in water between pH 1.7 and 2.7 (Figure S9, Supporting Information).

The cyclic voltammetry studies were carried out to explore the electrochemical behavior of **1** in 1 mol L^{-1} H_2SO_4 aqueous solution at 100 mV s^{-1} scan rate. In the potential range of 0.6 V to approximately −0.7 V, we can observe three pairs of reversible redox peaks, and the mean peak potentials ($E_{1/2}$ = $(E_{pa} + E_{pc})/2$) are −0.31, −0.06, and 0.14 V vs SCE. The redox peaks could be ascribed to three consecutive two-electron process of Mo.[10] In addition, when the scan rate changes from 120 to 300 mV s^{-1}, the anodic peak (I) along with cathodic peak (I′) potentials remain unchanged. But their current values are varied with increasing scan rates. The anodic current values keep growing, and the corresponding cathodic peaks shift toward the negative direction. However, the peaks are quite low when the scan rate is less than 100 mV s^{-1}. We can observe that the reversible peak currents are proportional to the scan rate, which illustrates that the redox process for **1** is surface controlled.[11]

Proton conductivity is a significant parameter that is widely applied in many areas, such as conductive materials, fuel cells, and electrochromic devices.[12] As known, heteropolyacids (HPAs) are ideal candidates as proton conducting electrolytes due to their unique characteristics of fast charge−transfer and abundant proton containers. Thus, we recorded the conductivity of **1**, as an example of original architecture beyond classical HPAs, in the temperature range of 30−100 °C. The values are estimated from the Nyquist plot (Supporting Information) and evaluated by $\sigma = L/(S \times R)$. At 30 °C, with 98% relative humidity (RH), the proton conductivity value of **1** is 7.58×10^{-4} S cm^{-1}, which is much higher than the value of well-known HPAs such as Keggin-type $[PMo_{12}O_{40}]^{3-}$ anions under the same conditions[13] or even higher than those untraditional POMs species, such as HMo_8W^{3-} derivatives, which represent the examples of a detailed study of ionic conductivity of alkali salts of polyoxomolybdate wheels.[14] With increasing temperature, proton conductivity values have grown rapidly and reached $2.19-2.55 \times 10^{-2}$ S cm^{-1} in the temperature range of 90−100 °C. The value is high and reveals the fine conductivity of **1**, even compared to the system of Nafion fuel cell membranes.[15] Figure 3a shows the Arrhenius plots of **1**, which are almost linear with increasing temperature, and the corresponding activation energy (E_a) value is 62.39 kJ mol^{-1} (0.647 eV), which is higher than 20 kJ mol^{-1}, indicating that the proton mechanism of **1** is a vehicle mechanism[16] attributed to the direct diffusion of the additional protons with water molecules.[12b] In addition, the proton conductivities of **1** were also measured at 30 and 100 °C with different RH values

dx.doi.org/10.1021/ic400848r | Inorg. Chem. 2013, 52, 8285−8287

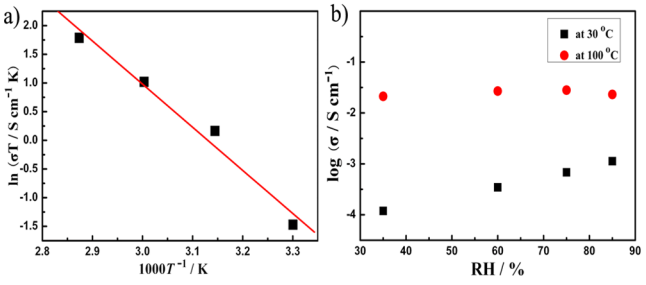

Figure 3. (a) Arrhenius plots of the proton conductivities of **1**. (b) Log σ (S cm^{-1}) versus RH plots of **1** at 30 and 100 °C.

(Figure 3b). We can observe that the conductivities of **1** at 100 °C are all higher than those at 30 °C. The values are increased with RH at 30 °C, while the conductivities at 100 °C remain nearly unchanged under different RH, which can show good conductive characteristics that are less sensitive to surrounding conditions.[17]

In conclusion, an unprecedented crown-shaped 24-molybdo-12-phosphonate, which is constructed by ATMP, has been synthesized by the conventional method. Compound **1** is the first example of a polyoxomolybdate ensemble built from functionalized triphosphonates. The high proton conductivity of **1** can provide a new organic−inorganic hybrid candidate in the field of material science. Future work will focus on the syntheses of more novel structures based on triphosphonates and studies of more potential properties of these compounds.

■ ASSOCIATED CONTENT

Supporting Information

X-ray crystallograhic files (CIF), experiment sections, synthetic discussion, additional physical measurements, and additional structural figures for **1**. This material is available free of charge via the Internet at http://pubs.acs.org.

■ AUTHOR INFORMATION

Corresponding Author

*E-mail: jyniu@henu.edu.cn (J.N.), jpwang@henu.edu.cn (J.W.).

Notes

The authors declare no competing financial interest.

■ ACKNOWLEDGMENTS

We gratefully acknowledge the National Natural Science Foundation of China, Foundation of Education Department of Henan Province, and Natural Science Foundation of Henan Province.

■ REFERENCES

(1) (a) Hill, L. M. R.; Abrahams, B. F.; Young, C. G. *Chem.—Eur. J.* **2008**, *14*, 2805−2810. (b) Nyman, M.; Burns, P. C. *Chem. Soc. Rev.* **2012**, *41*, 7354−7367. (c) Noro, S.-I.; Tsunashima, R.; Kamiya, Y.; Uemura, K.; Kita, H.; Cronin, L.; Akutagawa, T.; Nakamura, T. *Angew. Chem., Int. Ed.* **2009**, *48*, 8703−8706.

(2) (a) Stracke, J. J.; Finke, R. G. *J. Am. Chem. Soc.* **2011**, *133*, 14872−14875. (b) Uehara, K.; Mizuno, N. *J. Am. Chem. Soc.* **2011**, *133*, 1622−1625.

(3) (a) Banerjee, A.; Bassil, B. S.; Röschenthaler, G.-V.; Kortz, U. *Chem. Soc. Rev.* **2012**, *41*, 7590−7604. (b) Dolbecq, A.; Mialane, P.; Sécheresse, F.; Keita, B.; Nadjo, L. *Chem. Commun.* **2012**, *48*, 8299−8316. (c) Breen, J. M.; Schmitt, W. *Angew. Chem., Int. Ed.* **2008**, *47*, 6904−6908. (d) Finn, R. C.; Burkholder, E.; Zubieta, J. *Chem. Commun.* **2001**, 1852−1853. (e) Niu, J. Y.; Zhang, X. Q.; Yang, D. H.; Zhao, J. W.; Ma, P. T.; Kortz, U.; Wang, J. P. *Chem.—Eur. J.* **2012**, *18*, 6759−6762. (f) Kortz, U.; Pope, M. T. *Inorg. Chem.* **1995**, *34*, 3848−3850. (g) Banerjee, A.; Bassil, B. S.; Röschenthaler, G. V.; Kortz, U. *Eur. J. Inorg. Chem.* **2010**, *26*, 3915−3919.

(4) (a) Mayer, C. R.; Marrot, J.; Sécheresse, F. *J. Mol. Struct.* **2004**, *704*, 59−62. (b) Carraro, M.; Sartorel, A.; Scorrano, G.; Maccato, C.; Dickman, M. H.; Kortz, U.; Bonchio, M. *Angew. Chem., Int. Ed.* **2008**, *47*, 7275−7279. (c) Kortz, U.; Marquer, C.; Thouvenot, R.; Nierlich, M. *Inorg. Chem.* **2003**, *42*, 1158−1162. (d) Stalick, J. K.; Quicksall, C. O. *Inorg. Chem.* **1976**, *15*, 1577−1583. (e) Chubarova, E. V.; Klöck, C.; Dickman, M. H.; Kortz, U. *J. Clust. Sci.* **2007**, *18*, 697−710.

(5) (a) Finn, R. C.; Burkholder, E.; Zubieta, J. *Chem. Commun.* **2001**, 1852−1853. (b) Armatas, N. G.; Ouellette, W.; Whitenack, K.; Pelcher, J.; Liu, H. X.; Romaine, E.; O'Connor, C. J.; Zubieta, J. *Inorg. Chem.* **2009**, *48*, 8897−8910. (c) Burkholder, E.; Golub, V.; O'Connor, C. J.; Zubieta, J. *Inorg. Chem.* **2004**, *43*, 7014−7029. (d) Burgomaster, P. D.; Aldous, A.; Liu, H. X.; O'Connor, C. J.; Zubieta, J. *Cryst. Growth Des.* **2010**, *10*, 2209−2218.

(6) Ouellette, W.; Wang, G. B.; Liu, H. X.; Yee, G. T. *Inorg. Chem.* **2009**, *48*, 953−963.

(7) Müller, A.; Beckmann, E.; Bögge, H.; Schmidtmann, M.; Dress, A. *Angew. Chem., Int. Ed.* **2002**, *41*, 1162−1167.

(8) Peloux, C.; du Dolbecq, A.; Mialane, P.; Marrot, J.; Sécheresse, F. *Dalton Trans.* **2004**, 1259−1263.

(9) Robert, F.; Leyrie, M.; Hervé, G.; Tézé, A.; Jeannim, Y. *Inorg. Chem.* **1980**, *19*, 1746−1752.

(10) (a) Meng, J. X.; Lu, Y.; Li, Y. G.; Fu, H.; Wang, E. B. *CrystEngComm.* **2011**, *13*, 2479−2486. (b) Kan, W. Q.; Yang, J.; Liu, Y. Y.; Ma, J. F. *Inorg. Chem.* **2012**, *51*, 11266−11278.

(11) (a) Wang, B. X.; Dong, S. J. *J. Electroanal. Chem.* **1992**, *328*, 245−257. (b) Du, D. Y.; Qin, J. S.; Li, Y. G.; Li, S. L.; Lan, Y. Q.; Wang, X. L.; Shao, K. Z.; Su, Z. M.; Wang, E. B. *Chem. Commun.* **2011**, *47*, 2832−2834.

(12) (a) Thanganathan, U. *J. Mater. Chem.* **2011**, *21*, 456−465. (b) Daiko, Y.; Matsuda, A. *J. Jpn. Pet. Inst.* **2010**, *53*, 24−32.

(13) (a) Wei, M. L.; Wang, X. X.; Duan, X. Y. *Chem.—Eur. J.* **2013**, *19*, 1607−1616. (b) Wei, M. L.; Zhuang, P. F.; Li, H. H.; Yang, Y. H. *Eur. J. Inorg. Chem.* **2011**, 1473−1478.

(14) (a) Peloux, C. D.; Dolbecq, A.; Barboux, P.; Laurent, G.; Marrot, J.; Sécheresse, F. *Chem.—Eur. J.* **2004**, *10*, 3026−3032. (b) Dolbecq, A.; Peloux, C. D.; Auberty, A. L.; Mason, S. A.; Barboux, P.; Marrot, J.; Cadot, E.; Sécheresse, F. *Chem.—Eur. J.* **2002**, *8*, 350−356.

(15) (a) Kreuer, K. D.; Paddison, S. J.; Spohr, E.; Schuster, M. *Chem. Rev.* **2004**, *104*, 4637−4678. (b) Wei, M. L.; Zhuang, P. F.; Miao, Q. X.; Wang, Y. *J. Solid State Chem.* **2011**, *184*, 1472−1477. (c) Alberti, G.; Casciola, M. *Solid State Ionics* **2001**, *145*, 3−16.

(16) Tong, X.; Wu, X. F.; Wu, Q. Y.; Zhu, W. M.; Cao, F. H.; Yan, W. F. *Dalton Trans.* **2012**, *14*, 9893−9896.

(17) Wei, M. L.; Li, H. H.; Wang, X. X. *J. Clust. Sci.* **2012**, *23*, 325−344.